Tribological Analysis of Glass Fibers Using Atomic Force Microscopy (AFM)/Lateral Force Microscopy (LFM)

N. BEHARY, A. GHENAIM, A. EL ACHARI, C. CAZE

GEMTEX, Ecole Nationale Supérieure des Arts et Industries Textiles, 2, Place des Martyrs de la Résistance, F-59070 France

Received 21 November 1998; accepted 5 June 1999

ABSTRACT: By using atomic force microscopy (AFM)/lateral force microscopy (LFM), a comparative study of the topography as well as the tribological properties (at a micrometer scale) of sized E-glass fibers was done. Normal and lateral deflection signals are recorded when an AFM tip scans a fiber surface. Friction force data were obtained from the forward and backward scans of lateral force images whose contrasts reveal differences in friction coefficient values and, hence, surface chemical heterogeneity of certain-sized glass fibers. Sizes having an epoxy film former lead to a higher friction coefficient value than those containing a starch film former. Moreover, the epoxy-containing size is more readily plowed by the AFM tip. Annealing of this size lowers its friction coefficient. © 2000 John Wiley & Sons, Inc. J Appl Polym Sci 75: 1013–1025, 2000

Key words: glass fibers; size; atomic/lateral force microscopy; friction

INTRODUCTION

Glass fibers readily suffer abrasion damage due to friction when filaments slide against each other. In the absence of a suitable coating, friction leads to wear and fracture. In industries, glass fibers are coated with a size consisting of a coupling agent, a lubricant, a film former, and other additives. While the coupling agent is used to increase adhesion between the fibers and the matrix, in glass fiber-reinforced composite materials,[1,2] the complete size improves the tribological performance of contacting fiber surfaces during fiber processing and uses (e.g., weaving).

Tribology is a new term of the last two decades combining friction, adhesion, lubrication, and wear. It deals with the science of interacting materials in relative motion.[3,4] Knowledge of the tribological properties of glass fibers at microscopic and atomic levels is essential to understand friction at the macroscopic level. In this article, we will deal with microscopic friction only. The atomic force microscopy/lateral force microscopy (LFM/AFM), which provides, simultaneously, the surface topography and friction forces,[5] can be an invaluable probe for the study of fiber tribology.

Theory of Friction at Macroscopic Level

At the macroscopic scale, Amonton's law was one of the first theories established to describe sliding friction analytically[6,7]:

$$\text{Friction coefficient: } \mu = F_f/N$$

where μ is the coefficient of friction; F_f, the frictional force; and N, the normal applied force. Frictional forces depend both on the *surface roughness* as well as the *chemical nature* of the sliding substances.

Surface Roughness

At this scale, the frictional force (F_f) is independent of the apparent contact surface but is related

Correspondence to: C. Caze.

Journal of Applied Polymer Science, Vol. 75, 1013–1025 (2000)
 CCC 0021-8995/00/081013-13

to the true area of contact (A) such that $F_f = SA$ (where S is the shear strength per unit area), if neither of the two surfaces is soft.[6,8] Even plane surfaces are never perfectly flat as they always have a certain degree of roughness, such that contact occurs at discrete contact points. Indeed, at a macroscopic level and for a constant load (and assuming that no plastic deformation occurs), the greater the true contact area (A) where the apexes of asperities touch, so will be the frictional force, which is the force required to shear the junctions at the actual contact points (the plowing actions being neglected). Thus, surfaces having the same chemical composition but different roughness would have different coefficients of friction if the sliding load is of the same nature.

Several methods have been used to measure contours of the surfaces: profilometer, oblique sections, optical interference method, electron diffraction, and scanning electron microscopy (SEM). The AFM, invented by Bining,[9] allows one to measure from the surface topography the surface roughness corresponding to variations in the height of the surface relative to a reference plane.

However, the AFM tip sliding on a surface simulates only one such contact.[10] Any friction force variation at such a contact arises from a variation in the chemical nature.

Chemical Nature (of Polymeric Materials)

For polymeric materials, there is deviation from the Amonton's law because, in addition to the surface roughness, the frictional force will depend on the adhesion properties of the sliding surfaces and, hence, on the chemical nature (plasticity, viscoelasticity, and surface tension) of the polymer chains. For example, sliding is easier on *Teflon* than on *rubber*.

In the case of fibers and polymers, Tabor[6] and Bowden and Tabor[11] demonstrated that the determination of the coefficient of friction is not so simple, because, first, plastic or viscoelastic deformation may alter considerably the true contact area and, second, there may be plowing of a hard surface (e.g., a metal) on a softer one (e.g., polymers).

Friction of Fibers at Macroscopic Level

In fact, only in recent years has a more basic investigation been made on the frictional behavior of fibers. The most striking characteristic is that the coefficient of friction (μ) increases as the load (N) is diminished, and at light loads, it can be very high. Indeed, other than deformation at asperities observed in the fiber, the radius of curvature of the surface is an important parameter in determining friction.[11] Recently, Gupta[8] described the friction of fibers in empirical terms:

$$F_f = aN^n$$

where a and n are constants.

EXPERIMENTAL

Products

Sized glass fibers were supplied by Owens Corning (Belgium) in the form of roving, each containing 800 filaments of radius 11 μm. Fibers coated with five different sizes: A, B, D, E4, and F, were studied. These are used for the manufacture of a woven material used to reinforce composite materials. Each fiber sizing is composed of a film former, lubricants, additives, and a coupling agent. In all the cases, the coupling agent is an organosilane. However, as far as the film former is concerned, it is composed of starch for sizes A, B, and D, while for E4 and F, it is of an epoxy nature. For a same film former, sizes differ by their chemical composition, which remains confidential. In this article, we will call fibers by the name of the size that they contain.

AFM/LFM

The atomic force microscope (AFM), which was invented by Bining et al. in 1986,[9] is capable of measuring surface roughness from the topographic image obtained in the AFM mode and the microscopic friction forces down to nanometric scale in the LFM mode (Meyer and Amer, 1990, ref. 12). Extensive reviews already have dealt with this subject: Only a brief explanation of the functioning of the apparatus will be given in this article.

AFM Mode

AFM imaging was achieved in air under atmospheric conditions with a commercial scanning probe, Nanoscope III, from Digital Inc., in the contact mode, at a constant preset force. The AFM measures the vertical deflection of a cantilever to which is fixed a microtip which scans the sample

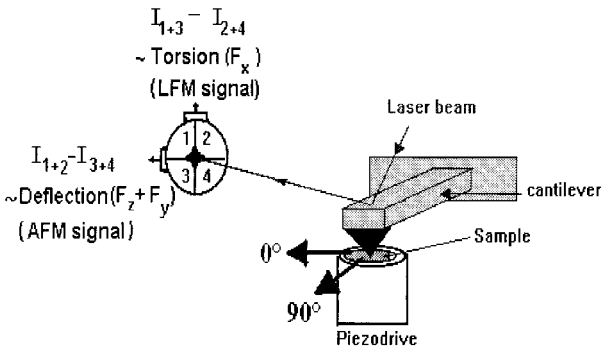

Figure 1 Principle of simultaneous measurement of the normal and lateral forces; two scanning directions are possible (0° and 90°).

surface (Fig. 1). The normal deflection of the cantilever is such that $F_z = k \times z$, where F_z is the deflection force; k, the spring constant of the cantilever; and z, the cantilever's deflection. This deflection is due to intermolecular forces (attractive and/or repulsive), and in the contact mode, repulsive forces, which are dependent on the distance between the tip and the sample, are involved.

The sample is placed onto a piezodrive, while the tip is in a fixed position. It is the sample that is displaced underneath the AFM tip, so as to prevent any influence of external vibrations on the results. The normal deflection of the cantilever is monitored through the displacement of a laser beam reflected off the cantilever onto a segmented detector during the scanning of the sample in the x and y directions (Fig. 1). Any bending of the cantilever due to bumps or grooves on the sample surface induces an intensity difference between the lower and upper parts of the segmented photodetector, and this, in turn, provides an error signal for the feedback of the piezo so as to maintain a constant preset force on the cantilever. The displacement of the piezodrive allows one to reconstitute the topographic image of a scanned surface.

LFM Mode[3]

The lateral force images were obtained by measuring the torque imposed on the cantilever by the tip as a result of tangential forces [F_x: Fig. 2(B)] experienced by the tip when the sample is moved underneath it. To measure normal and lateral forces simultaneously, a four-quadrant photodiode is used (Fig. 1). The normal bending of the cantilever is measured by the intensity difference ($I_{1+2} - I_{3+4}$) of the upper and lower segments of the diode, while the signal difference of the left and the right segments ($I_{1+3} - I_{2+4}$) provides torsional information.

Topographic and LFM images

Topographical 3-dimensional as well as scope-mode images were obtained in the AFM and LFM modes. Scope-mode images give trace and retrace profiles, in real time, when the sample goes forward and backward underneath the tip. In the topographic mode (height), the two lines should merge into one another. If this is not the case, then false measurements would be taken, as a result of tip wear-out or as a result of a badly fixed sample. In addition to visual analysis, mean roughness may be calculated once the captured cylindrical form image of the fiber has been flattened using a planefit parameter.

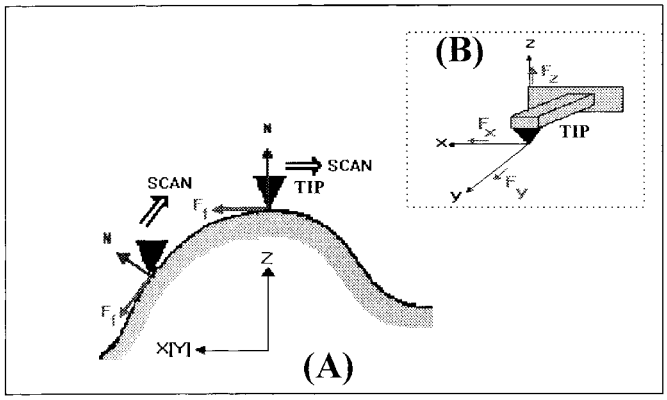

Figure 2 (A) Normal reacting force (N) as well frictional force (F_f) acting on a surface with corrugations; (B) schematic presentation of the X, Y, and Z components of the forces acting at the top of the cantilever

LFM trace and retrace images give the lateral force signals (corresponding to the topographic image) when the sample goes forward and backward underneath the tip. The distance separating the trace and retrace lines in the scope mode give information concerning the friction force at a constant contact force.

Classification of AFM/LFM Images and Measurement of Friction Force from Lateral Force Signals

At first, topography and lateral forces were interpreted as real-surface topography and frictional force, respectively, that is, the origins of the deflection of the cantilever due to topographic effects were attributed to the z and y components of the tip-deflection force: F_z and F_y only [Fig. 2(B)], whereas the torsion (F_x) of the cantilever was attributed to the frictional force between the sample surface and the tip only. But trippings caused by bumps or grooves owing to the surface topography were observed in the lateral-force images.

Fujisawa and Sugarawa[13] worked on the influence of topography on the lateral-force signal. They showed that for an atomically flat surface with friction the frictional force (F_f) contibutes to F_x and F_y [Fig. 2(B)] and the normal reacting (N) force contributes to F_z only. But for a frictionless surface with corrugations, the normal reacting force (N) has nonzero x, y, and z components and, thus, contributes to the F_x, F_y, and F_z.

For a surface with friction as well as with corrugations [Fig. 2(A)], like the glass fibers used in this study, the normal reacting force (N) as well the frictional force (F_f) will have nonzero x, y, and z components, that is,

$$N = N_x + N_y + N_z$$

$$F_f = F_{fx} + F_{fy} + F_{fz}$$

In other words, the measured lateral force depends on the local slope as well and not only on frictional forces. Moreover, meniscus forces may also influence the lateral force.

The friction force (F_f) is, of course, tangent to the slope [Fig. 2(A)] and acts in the opposite direction to the scan direction, and, therefore, by the reversal of the scan direction, each of the components of the frictional force (F_f) changes sign, while those due to the normal force do not. Thus, each of the lateral force signals (F_x) measured in the opposite scan directions is such that

The forward scan LFM signal: $F_x = N_x + F_{fx}$

and

The backward scan LFM signal: $F_x = N_x - F_{fx}$

The difference between the forward and the reverse scans in the LFM scope mode gives twice the average friction force (Overney and Meyer[3]; Baselt and Baldeschwielder[14]). Full quantification of the frictional force is not yet possible, but it is assumed that scanning at 90° (Fig. 1) cancels the y and z components of the friction force.

Sample Preparation

Sized glass filaments were provided by Owens Corning in the form of multifilament rovings. One or several of the filaments were fixed onto a double-face Scotch tape, perpendicularly to the scan direction (90°), so as to measure both topographic and frictional data.

This perpendicular position enables one to see in the scope mode the exact position of the fiber with respect to the tip point. As the maximum of the piezodrive in the z direction is limited to 5.9 μm, the fiber cannot be scanned wholly. So, only the most elevated part of the fiber, where the slope (or curvature) is minimum, was rastered.[15] Indeed, we shifted from a 6×6 to a 3×3-μm^2 surface by zooming the top of the fiber, in the image mode, in real-time.

A "J" head with scan area of 130×130 μm^2 was used. Conical-shaped ultralevers made from silicon nitride and attached to the cantilever (180 μm long) with a spring constant $k = 0.06$ N/m were used. Samples were rastered at a constant force between 20 and 90 nN. Topographic and lateral force images were obtained at a scan rate of 1.12 Hz with 512 samples per area scanned.

Force Calibration

Indeed, force calibration is necessary in order to determine the normal contact force acting on the surface sample. For this, the X and Y voltages of the piezodrive (Fig. 1) are held at zero and a waveform voltage is applied to the Z electrode. As a result, the sample moves up and down relative to the stationary cantilever tip, and, simulta-

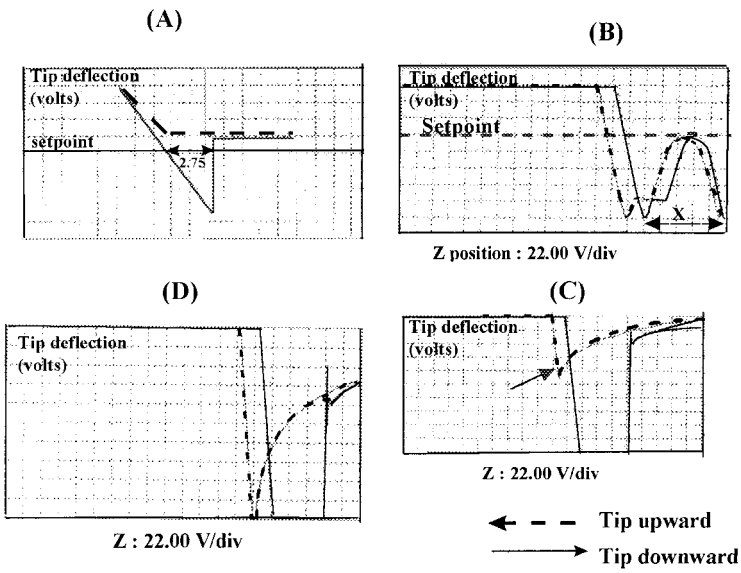

Figure 3 (A) A normal contact force curve profile. Contact force curve profile during scanning of (B) fiber E4, (C) fiber F, and (D) a desized glass fiber.

neously, the cantilever deflection signal from the photodiode is monitored. Figure 3(A) depicts a typical force curve representing the deflection signal for one complete upward and downward movement cycle of the piezo. The set point is the value at which the deflection signal is maintained.

The normal contact force is then calculated by the equation

$$F_z = k\Delta z$$

where Δz is the distance from the control point to the pull-off point of the tip [indicated by arrows in Fig. 3(A)] in nanometers. An example of computation of the contact force is given below:

$$F_z = k\Delta z$$

where $K = 0.6$ N/m (spring constant). According to Figure 3(A),

The Z piezo sensitivity being $Sz = 2$ nm/v,
$\Delta z = 2.75$ div $\times$ 10.0 V/div $\times$ 2 nm/V = 55 nm,
Normal force = $N = 0.6$ N/m $\times$ 55 nm = 33nN.

As far as the lateral force is concerned, it is measured in volts by the LFM mode. Several methods of lateral force calibration have been proposed. The methods of Ruan and Bhushan[16] and of Marti[17] are well known. With the former requiring additional equipment (electronic scanning microscope), we opted to use the calibration method of Marti, which, although not very precise, is easy to use if the average dimensions of the tip and the cantilever is known. The average sensitivity of the lateral force S_{lat} in nN/V was calculated to be around 40 nN/V.

RESULTS AND INTERPRETATIONS

Images obtained in the AFM mode (topography) and in the LFM mode are presented. The difference between the LFM backward and forward signals gives twice the friction force in volts. Friction coefficients were calculated by dividing the friction force (in nN) by the normal applied force (in nN), the latter being calculated and calibrated by using the contact force curve profile, as described earlier. For each fiber, numerous tests were performed and the friction coefficient values were found to be reproducible when tests were carried out on different regions of a filament as well as on different filaments of the same glass fiber.

The friction coefficient values were found to be relatively small and varied from 0.01 to 2. These are relevant values, especially when we compare them to those obtained by other authors who worked on polymeric films and other surfaces (see

Table I Microscale and Macroscale Friction Coefficient Data of Different Surfaces

Films	LFM Friction Coefficient (Si_3N_4) Tip	Film/Film (PET) Friction Coefficient
PET films[18]		
A	0.06	0.71
B	0.04	0.77
C	0.04	0.66
Hydrogenated carbon films[19]	0.02–0.04	—
Various Samples[16]		Macroscale Friction Coefficient Measurements with Si_3N_4 Ball
Platinum	0.054	0.3
Aluminum	0.08	0.6
HOP graphite	0.006	0.1

Table I). As compared to macroscale friction coefficient values, microscale friction coefficients are relatively small.

Results of Fibers Coated with a Size Containing Starch Film Former

Fiber A

Images obtained in the AFM and LFM modes have been realized at a contact force of 38 nN (Fig. 4). The topographic image [Fig. 4(A)] shows randomly distributed bumps of variable dimensions. The forward and backward scanned images in the LFM mode corresponding to the topographic image of Figure 4(A) are presented in the Figure 4(B). They show that contrasts on the bumps are reversed when the scanning direction is changed. The scope mode AFM and LFM signals of sections A–A′ and B–B′ corresponding to extremities of the topographic image of Figure 4(A) are illustrated by Figures 3(C,D), respectively. The scope-mode LFM signals of both sections reveal on the bumps a friction force (F_f) of $\approx$ 0.035 V (indicated by full lines), that is, a friction coefficient $\mu \approx 0.04$, while the remaining surface (indicated by dashed lines) has a friction force two to three times greater, that is, a friction coefficient $\mu \approx 0.12$. Furthermore, we can also observe in the LFM mode that in each of the two regions there are small fluctuations of the backward and forward signals. We have then chosen to determine friction forces by considering the average value of the signals only. The glass fiber of size A presents, therefore, a physically and chemically heterogeneous surface, with bumps having a friction coefficient $\mu \approx 0.04$, while the overall surface has a friction coefficient $\mu \approx 0.12$.

Fiber B

Scanning of the fiber of size B was done at a normal contact force of 86 nN. A particular illustration of its topographic image is given by Figure 5(A). We can hardly distinguish three distinct regions from the scope-mode LFM signals of section C–C′ [Fig. 5(B)], corresponding to bottom section of the topographic image in Figure 5(A):

- Region 1: $F_f \approx 0.015$ V, that is, $\mu \approx 0.007$ (full dark line);
- Region 2: $F_f \approx (2.5–3) \times 0.015$ V, that is, $\mu \approx 0.02$ (dashed dark line);
- Region 3: $0.015 \text{ V} < F_f < (2.5–3) \times 0.015$ V, that is, $\mu \approx 0.007–0.02$ (gray line).

In the case of this fiber, the friction coefficients are independent of the surface topography, that is, it is difficult to attribute a particular friction coefficient to a particular feature (bumps, hollows, or plane surface). However, in spite of the differences among the friction coefficients in the three different regions, their values remain, in general, very small (maximum friction coefficient value &mg; $\approx$ 0.02). Moreover, the backward and forward scanned images in the LFM mode (not illustrated here) show that changing the scanning direction does not reverse the image contrasts. This is, indeed, the case of surfaces having a very weak friction coefficient, for example, lubricated surfaces, as was shown by Fujisawa and Sugarawa.[13]

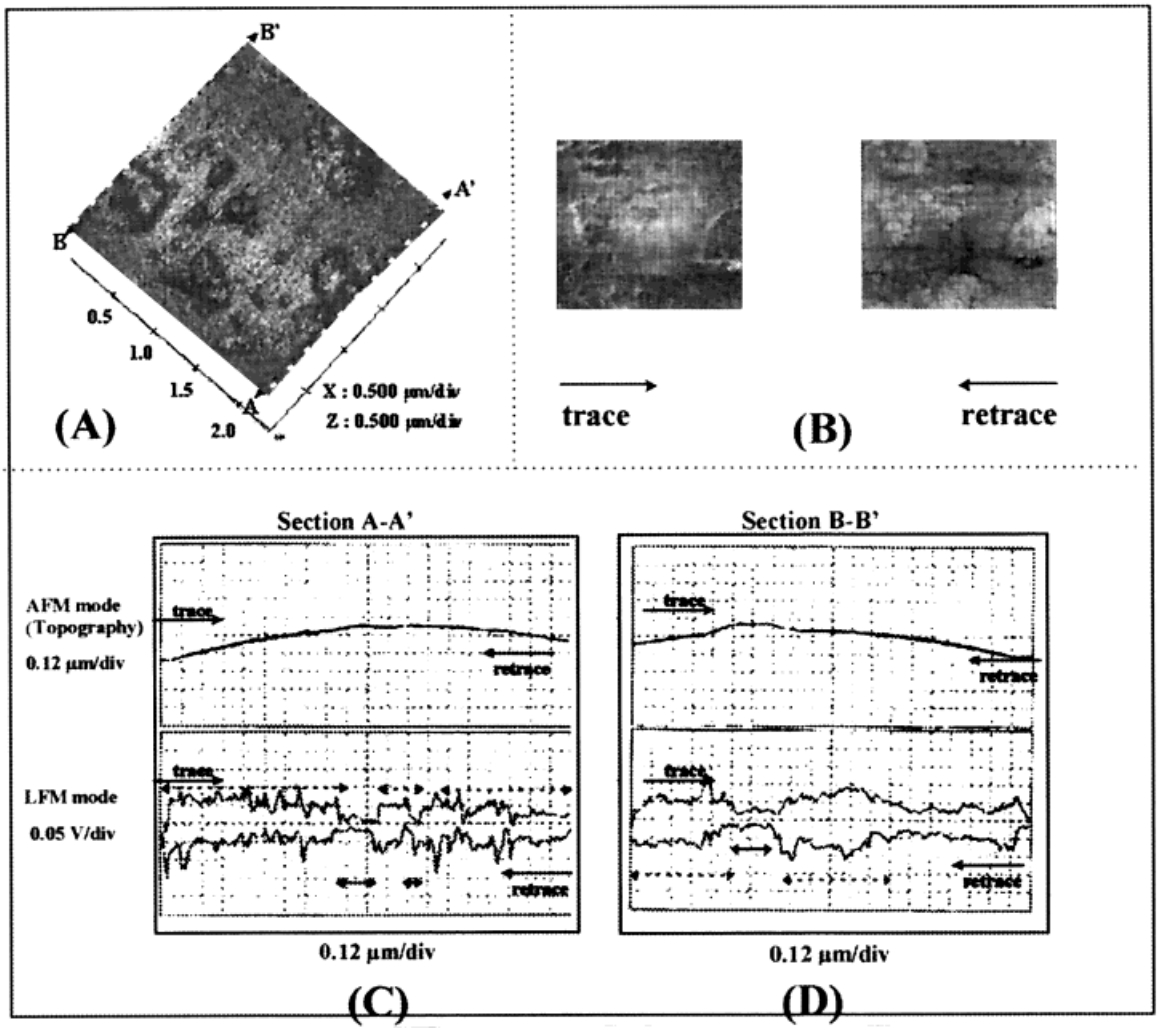

Figure 4 Fiber A: (A) topographic image; (B) forward and backward scanned LFM images; (C) scope-mode forward and backward scanned AFM and LFM signals of section A–A′; (D) scope-mode forward and backward scanned AFM and LFM signals of section B–B′.

Fiber D

On topographic images of fiber D, big bumps and small blisters could be observed. LFM signals corresponding to the topographic images showed small fluctuations of the friction coefficient which varied in the range of 0.05–0.08. These are relatively small values. The friction force of the blisters could not be differentiated from that of the remaining surface.

As far as the bumps are concerned, these are separated from each other by a distance greater than that existing between two blisters. A typical topographic image of fiber D in Figure 6(A) shows a 0.2-μm high bump. The scope-mode forward and backward AFM and LFM signals across this bump [Fig. 6(A)] allows one to calculate its friction coefficient, which is approximately the same as the general surface: $\mu \approx 0.05–0.08$. The great fluctuations of the LFM signals at positions indicated by crosses are due to the influence of the bump slopes on the AFM tip, during forward and backward scanning. To summarize, the surface of the glass fiber of size D is characterized by bumps, blisters, and plane regions, all of them having a similar friction coefficient.

Results of Fibers Coated with a Size Containing an Epoxy Film Former

Fiber E4

In the topographic image [Fig. 7(A)] realized at a contact force superior than 70 nN, surface dam-

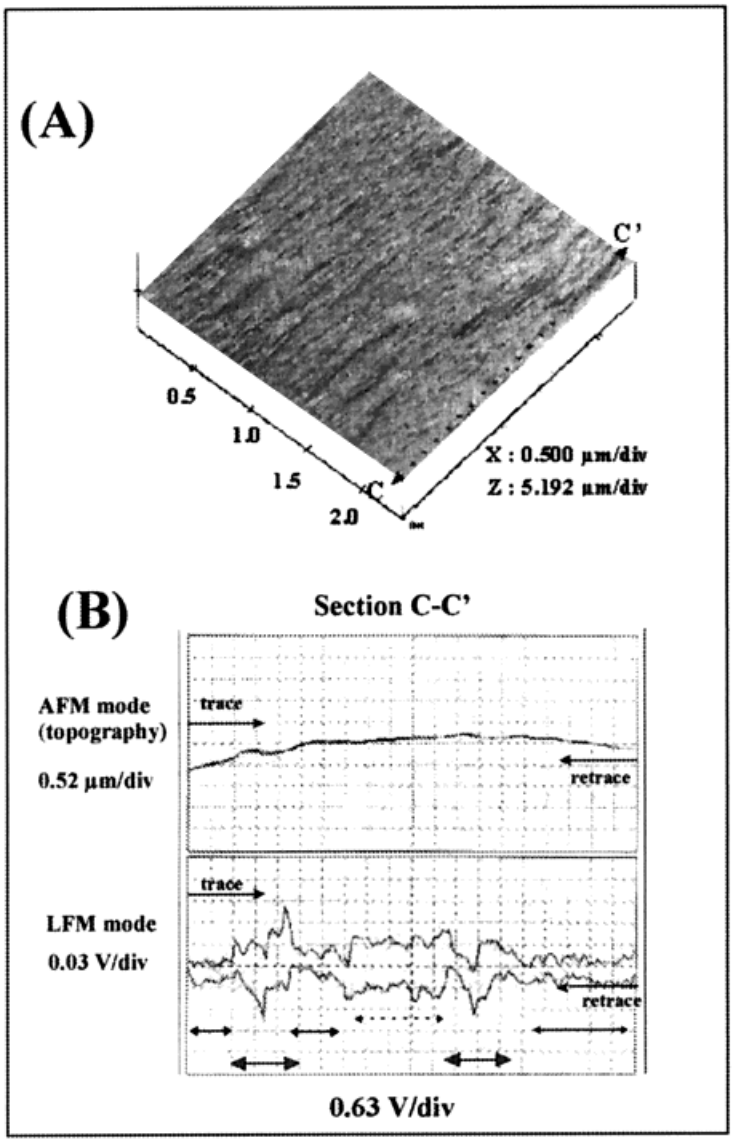

Figure 5 Fiber B: (A) topographic image; (B) scope-mode forward and backward scanned AFM and LFM signals of section C–C′.

age due to the plowing of size E4 by the AFM tip is observed. In many cases, topographic images could not be realized because of problems met in the calibration of the normal contact force. Indeed, as can be seen in Figure 3(B), the AFM tip remains "stuck" to the size in the region indicated by X, and it is difficult to pull-off the tip from the surface [the profile of a normal force calibration curve expected is shown in Fig. 3(A)]. In cases where the plowing phenomenon occurs, LFM signals such as those illustrated in Figure 7(B) are obtained. The difference between the forward and backward LFM signals is $\approx 2 \times 1.20$ V, which is a very high value compared to sizes with a starch film former (A, B, and D). This value remains constant all along section A–A′, in spite of the bump at the middle section.

The friction force is thus dependent on the normal applied force N and of the plowing force P, that is,

$$F_f = \mu N + P$$

The plowing phenomenon, which depends on the plowed surface area, is predominant and constant, so that the real friction coefficient of size E4 cannot be determined.

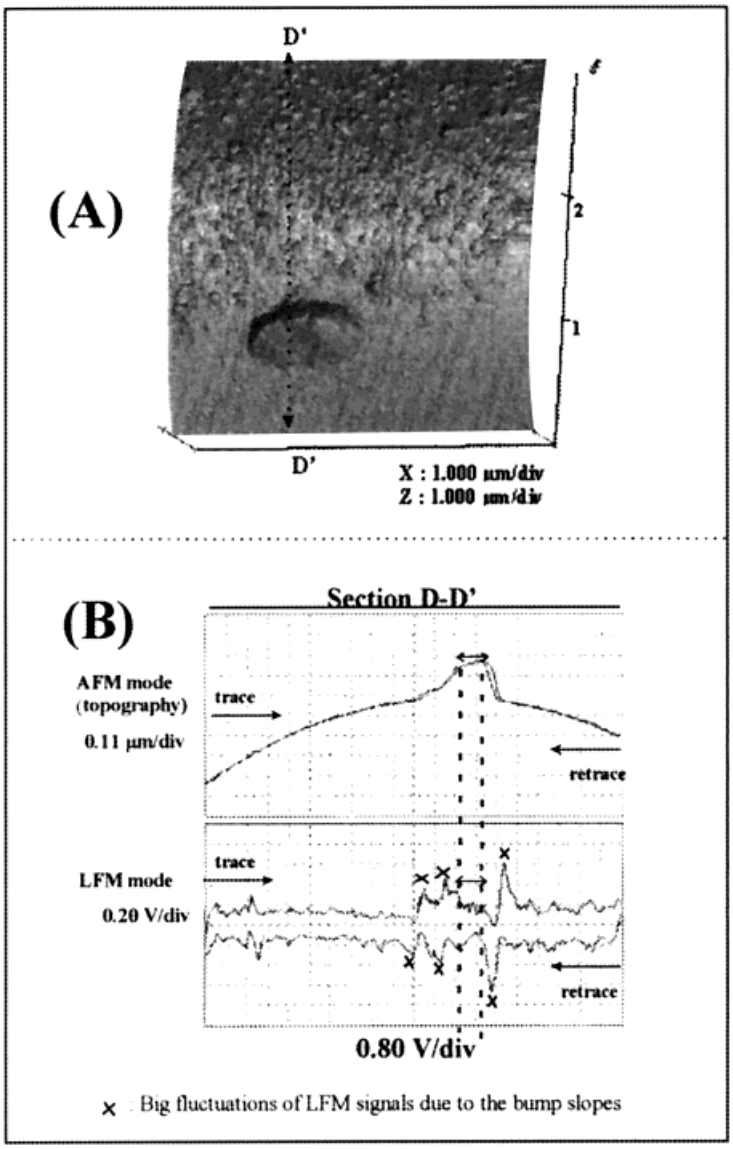

Figure 6 Fiber D: (A) topographic image; (B) scope-mode forward and backward scanned AFM and LFM signals of section D–D′.

Topographic images of other fibers taken from the same roving of fiber E4 showed that plowing did not occur although the same contact force was used. In these cases, the contact force curve profile was normal. The difference between the forward and backward LFM signals [in Fig. 7(B)] revealed a constant friction coefficient of 0.2 all over the fiber surface. This value is greater than those of fibers with a starch film former, for which the maximum friction coefficient is around 0.12. The fact that some fibers are readily plowed by the AFM tip while others are not may indicate a difference in the degree of crosslinking of the epoxy film former, among fibers of a same roving.

Fiber E41

This concerns fiber E4 annealed at 100°C for 60 h. The topographic image realized at 46 nN [Fig. 8(A)] does not present any plowing, and the contact force calibration curve profile was normal. Nevertheless, it reveals an aggregation of matter with the formation of small blisters (indicated by arrows) of a diameter of approximately 0.15 μm. LFM signals of a 1-μm^2 scanned area [Fig. 8(B)] allows us to determine the friction coefficient of a blister (full line) whose value $\mu \approx 0.03$ is smaller than that of the general surface for which $\mu \approx 0.09$.

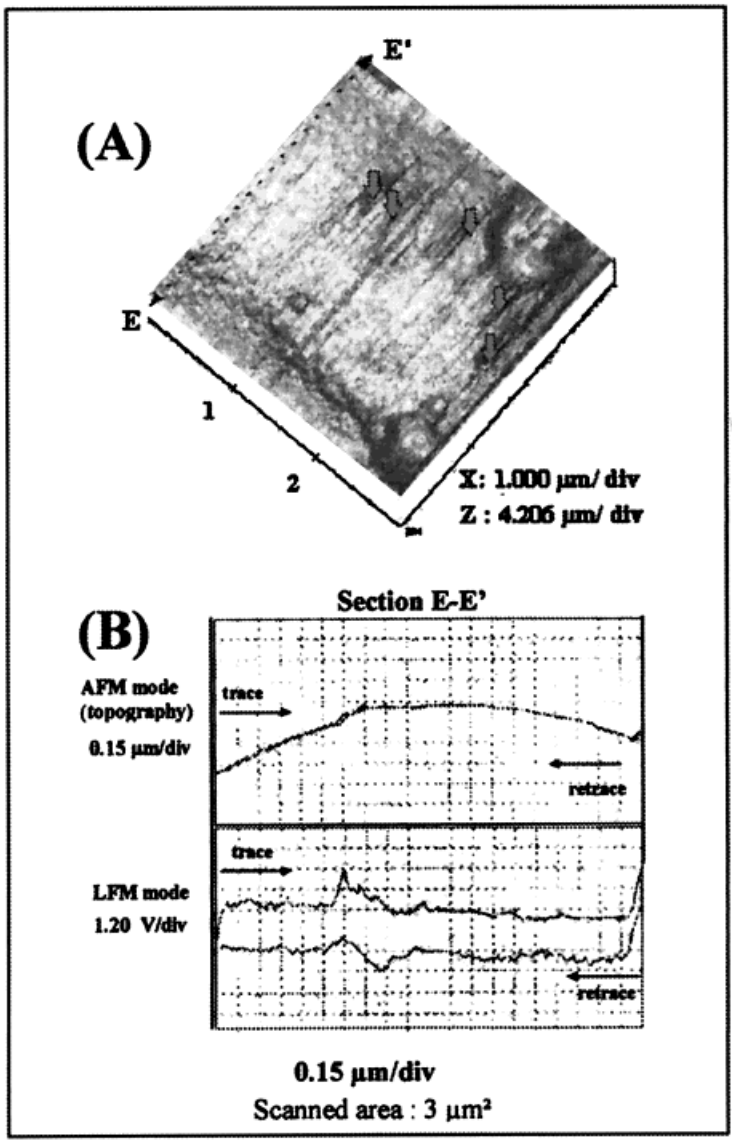

Figure 7 Fiber E4: (A) topographic image (plowing postions are indicated by arrows); (B) scope-mode forward and backward scanned AFM and LFM signals of section E–E′.

According to the observations made on the annealed glass fiber E4, in both the AFM and LFM modes, it can be said that The increased crosslinking of the epoxy resin by annealing leads to a sized surface having a higher surface Young's modulus. The size is therefore less susceptible to be plowed by the AFM tip. One can also propose the hypothesis that during an increased crosslinking of the epoxy film former the lubricant is expurgated off onto the external surface in the form of blisters. This would have, consequently, the effect of decreasing the coefficient of friction ($\mu \approx 0.03$).

Fiber F

Like fiber E4, F was also readily plowed by the AFM tip. An example of the topographic image realized at 60 nN and where plowing did not occur is shown in Figure 9(A). The forward and backward scanned LFM signals [Fig. 9(B)] show a heterogeneous surface, with a region having a coefficient of friction ≈ 0.05 on a distance of 0.3 μm (full line), while the remaining surface has a higher friction coefficient of 0.13 (a higher value). Moreover, the profile of the contact force curve shows that the AFM tip is attracted by size before

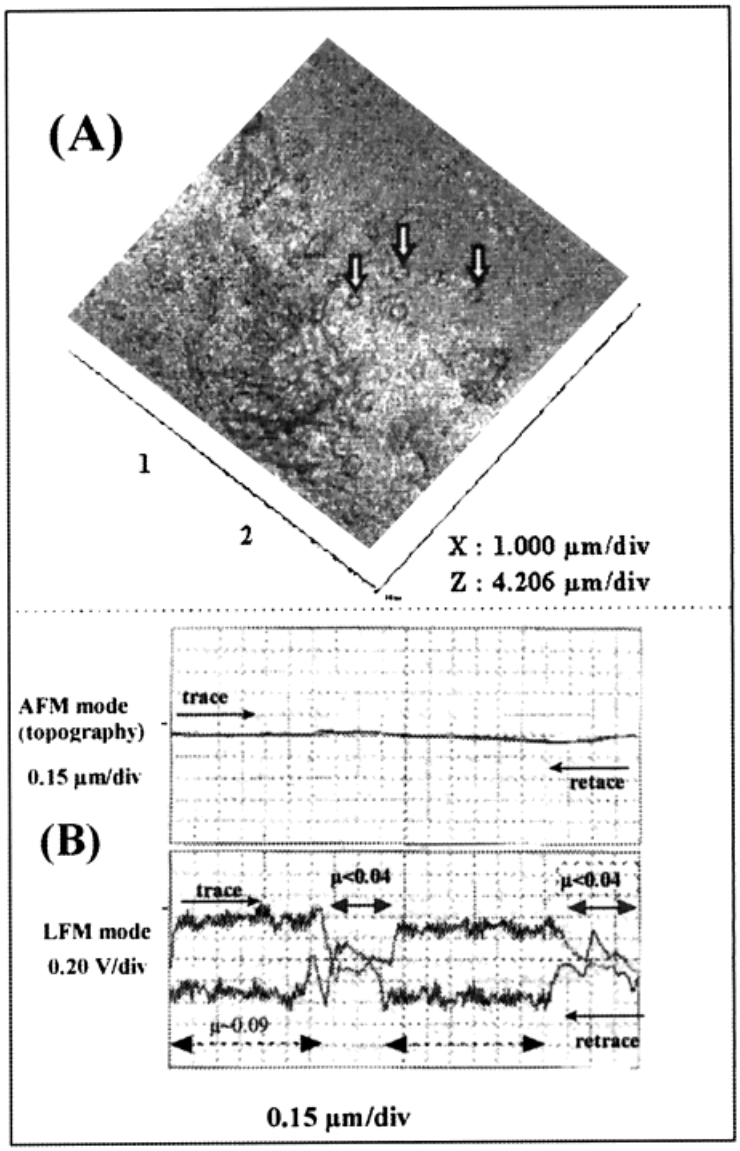

Figure 8 Annealed fiber E41: (A) topographic image; (B) scope-mode forward and backward scanned AFM and LFM signals.

its contact with the size [indicated by an arrow in Fig. 3(C)]. This phenomenon may be due to a great adherence between size F and the AFM tip. The difference between F and E4 is that the latter one has a homogeneous surface, while the former has a chemically heterogeneous surface.

Desized Glass Fiber

To analyze the glass fiber without any size, a desizing procedure was established. It consisted in heating the sized fiber at 600°C for 24 h so as to completely destroy the organic size. The topographic image of a desized glass fiber reveals a completely smooth surface. The coefficient of friction evaluated is very small, $\mu \approx 0.04$, and it remains constant all throughout the fiber surface. Moreover, one can note a great attraction of the tip by the sample before the former may be in contact with the fiber [dashed curve in Fig. 3(D)]. We explain this phenomenon by a higher surface energy of the clean desized glass fiber which is going to attract water molecules of the air very rapidly. Indeed, molecules of water form a film of water at the fiber surface, and this acts as a lubricant—hence, the very weak value of the fric-

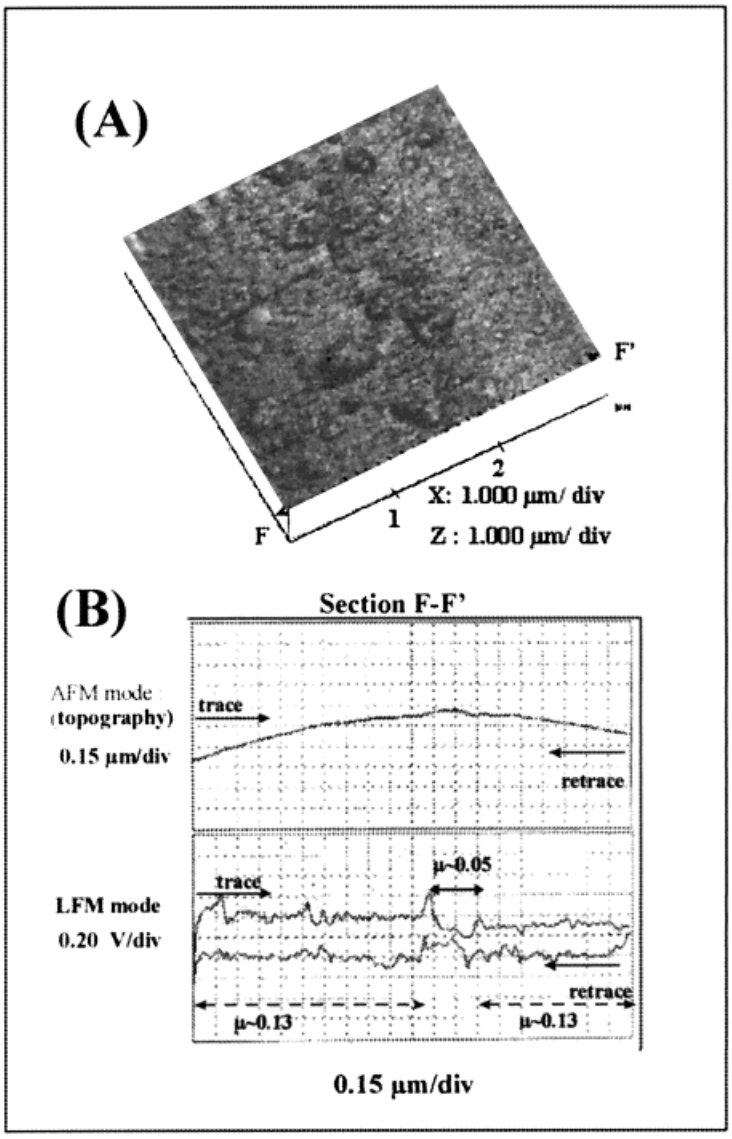

Figure 9 Fiber F: (A) topographic image; (B) scope-mode forward and backward scanned AFM and LFM signals of section F–F′.

tion coefficient. With the glass fiber surface being completely plain, we can conclude, therefore, that the chemical and physical heterogeneities on the fiber are brought about by sizing agents exclusively.

CONCLUSIONS

In the light of above discussions and results, it can be said that sizes having an epoxy film former lead to a higher friction coefficient value than do sizes containing a starch film former. Moreover, epoxy-containing sizes are readily prone to be plowed by the AFM tip: This implies that their surface modulus is smaller than that of starch-containing sizes. Nevertheless, on annealing the size, plowing effects decrease.

In addition to surface topography, chemical analysis of the fiber surface is possible from the friction coefficient values obtained in the LFM mode. Regions having a small friction coefficient ($\mu < 0.05$) may be due either to the overall size frictional nature (sizes B and D) or to a possible phase separation of the lubricant after size application on the fibers (sizes A and F).

The exact nature of friction in the fibers is known to be complex, and the lateral force between the probing tip of the AFM and a sample allows one to compare qualitatively different sizings and, in particular, their frictional properties. In the future, other fiber surfaces and their size or other coatings used in textile processing can be analyzed in the same way.

We would like to express our gratitude to V. Wolff from GEMTEX and Mr. W. Piret from Owens Corning for their support of this project.

REFERENCES

1. Clark, H. A.; Plueddeman, E. P. Mod Plast 1963, 40, 133–135.
2. Plueddemean, E. P. Silane Coupling Agents; Plenum: New York, 1982.
3. Overney, R., Meyer, E. Mrs Bull 1993, 18, 26–34.
4. Williams, J. A. Engineering Tribology; Oxford Science Publications: Oxford, 1994.
5. Lu, C.-J.; Miyamoto, T. Trans ASME 1995, 117, 334–342.
6. Adamson, A. W. Physical Chemistry; Wiley: New York, 1990; 460–489.
7. Howell, H. G.; Mazur, J. J Text Inst 1953, 44, T59–69.
8. Gupta, B. S. In Polymer and Fiber Science, Recent Advances; Fornes, R. E.; Gilbert, R. D., Eds.; Mark, H. F., Honorary Ed.; VCH: New York, 1992, pp 305–332.
9. Bining, G.; Quate, C. F.; Gerber, Ch. Phys Rev Lett 1986, 56, 930–933.
10. Bhushan, B.; Israelachvili, J. N.; Lman, U. Nature 1995, 374 , 607–616.
11. Bowden, F. P.; Tabor, D. Friction and Lubrication; Oxford University Press: London, 1956.
12. Meyer, E.; Amer, N. M. Appl Phys Lett 1988, 53, 1045–1047.
13. Fujisawa, S.; Sugarawa, Y. Microbeam Anal 1993, 2, 311–316.
14. Baselt, D. R.; Baldeshwielder, J. D. J Vac Sci Tech B 1992, 10, 2316–2322.
15. El Achari, A.; Wolff, V.; Ghenaim, A.; Caze, C. Text Res J 1996, 66, 483–490.
16. Rua, J.-A.; Bhushan, B. Trans ASME 1994, 116, 378–388.
17. Marti, O. Phys Scr T 1993, 49, 599–604.
18. Bhushan, B.; Koinkar, V. N. Trans ASME 1995, 38, 119–127.
19. Zhaoguo, J.; Lu, C. J. Thin Solid Films 1995, 258, 75–81.